PIBB 生物化学与生物物理进展
*Progress in Biochemistry and Biophysics*
2018, 45(4): 442~452
www.pibb.ac.cn

# Virtual Screening of Protein Tyrosine Phosphatase 1B Inhibitors Based on Natural Products

ZHANG Qian[1)], GAN Qiang[1)*], LIU Xia[2)], CHEN Xi[1)], FENG Chang-Gen[1)*]
([1)] *State Key Laboratory of Explosion Science and Technology, Beijing Institute of Technology, Beijing* 100081, China;
[2)] *College of Science, China Agricultural University, Beijing* 100193, China)

**Abstract** Protein tyrosine phosphatase 1B (PTP1B) is one of the targets of type Ⅱ diabetes, screening PTP1B inhibitors is of great significance. Structure-based virtual screening against a library of natural products containing 42 296 molecules was conducted to determine the occurrence of PTP1B inhibitors by molecular docking method. Firstly, the active sites of PTP1B complex crystal structure (PDB code: 1XBO) were analyzed and 7 amino acid residues, Arg254，Gln262，Tyr46，Asp181，Ser216，Phe182，and Arg221, were identified as the active pocket. Before docking, all the molecules were filtered according to the Lipinski's Rule of Five. Then, the screening was carried out based on the LibDock module and CDOCKER module, and 11 top-scored compounds were screened out as virtual hits. Of which 3 molecules, namely para-benzoquinone compound *7*, isocoumarins derivative *10* and Clavepictine analogue *11*, were determined with low toxicity ultimately according to the predictive ADME simulation and predictive toxic simulation. Binding model analysis revealed that these 3 candidate compounds are all good drug-like PTP1B inhibitors, of which the PTP1B inhibitory activity of compound *10* and *11* haven't been reported before, of which *in vitro* PTP1B enzyme inhibition of compound *10* was tested with $IC_{50}$ values of (74.58±1.23) μmol/L, which is potential for the treatment of type Ⅱ diabete.

**Key words** protein tyrosine phosphatase 1B inhibitors, virtual screening, natural products, pharmacokinetic characteristics, toxicological properties, hydrogen bonds, inhibitory activity
**DOI**: 10.16476/j.pibb.2018.0020

Protein tyrosine phosphatase 1B (PTP1B) is widespread in many tissues of human body, such as adipocytes, epithelial cells and so on. In 1990, it was demonstrated for the first time that PTP1B plays a negative regulatory role in insulin signaling through *Xenopus* oocyte experiments by Cicirelli *et al.*[1] In 1999, Elchebly[2] knocked out the PTP1B gene in mice, and revealed that PTP1B could be one of the targets for the treatment of type Ⅱ diabetes and obesity. So far, many kinds of PTP1B inhibitors with high activity and selectivity have been reported, which can be sorted into two categories according to their interaction sites, tyrosine phosphate analogues[3] and allosteric inhibitors[4], binding with the catalytic activity area and allosteric sites, respectively. In addition, some inhibitors' interaction sites aren't clear[5].

With the development of Computer Aided Drug Design (CADD), the cycle of drug research and development has greatly been shortened, contributing to the optimization of the molecular structure of inhibitors[6]. In 2005, Oh *et al.*[7] found the extracts from *Psidium guajava* could inhibit PTP1B activity and decrease the blood sugar in mice. Afterwards, Liu *et al.*[8] screened 32 compounds in *Psidium guajava*, obtaining 5 flavanoids and tannins compounds with PTP1B inhibitory activity. In 2009, Park *et al.*[9] screened chemical database containing 350 000 compounds, and identified 9 novel PTP1B inhibitors. In 2013, Joshi *et al.*[10] screened ZINC database by taking advantage of high-throughput screening technology and obtained one inhibitor, ZINC02765569. In 2015, two separate 3D quantitative structure-activity relationship models were constructed according to the dual inhibitors of aldose reductase (ALR2) and PTP1B, and were subsequently used as

*Corresponding author.
GAN Qiang. Tel: 86-10-68913770, E-mail: ganqiang@bit.edu.cn
FENG Chang-Gen. Tel: 86-10-68912941, E-mail: cgfeng@cast.org.cn
Received: January 15, 2018 Accepted: March 9, 2018

3D query search for virtual screening [11]. In 2016, Wang *et al*. [12] reported two novel ZINC01433265 derivatives compound-candidates, which could inhibit PTP1B activity by high throughput and virtual screening (HTS/VS) the ZINC Drug-like Database and structural optimization in silicon. Last year, Chandra *et al*. [13] utilized various machine learning techniques, such as naive Bayes along with molecular descriptors and structural fingerprints to construct models to search the Maybridge database and two compounds were found to have significant PTP1B inhibitory activity in experimental assay.

Up to now, at least 4 candidate drugs were proceeded to phase Ⅰ or phase Ⅱ clinical research, which include small molecule inhibitors Trodusquemine and Ertiprotafib [14], and antisense oligonucleotides PTP1B inhibitors ISIS-113715 and ISIS-PTP1BRx[15]. Unfortunately, no clinically applied PTP1B inhibitors are approved by FDA. It may be because most inhibitors reported have proven difficult to develop into drugs as a result of large molecular mass (>500u), high negative charges, low cell permeability, high lipophilic coefficient or poor bioavailability and selectivity[16-17]. Therefore, it is still important to develop new drugs targeting PTP1B for the treatment of diabetes and obesity.

In the present study, a library of natural products containing 42 296 small molecules was constructed. Structure-based virtual screening involving molecular docking simulations was performed to obtain the PTP1B inhibitors, combined with pharmacokinetic and toxicological properties screening. The binding modes between inhibitors and PTP1B were discussed. An accurate docking model and authenticated scoring functions were applied in the research, which would exert an important influence on increasing the hit rate in the docking. That simulations of pharmacokinetic and toxicological properties were helpful tools for forecasting the drug-likeness of the identified inhibitors.

## 1 Materials and methods

Molecular preparation, energy optimization, virtual screening and docking research were all performed within Discovery Studio 3.1 software distributed by the Accelrys company[18].

### 1.1 The preparation of PTP1B crystal structure

Crystal structure of PTP1B (PDB code: 1XBO) was selected from protein data bank (PDB)[19] (http://www.rcsb.org/) shown in Figure 1. Resolution of the crystal structure is 2.5Å, length is 435 and the relative molecular mass is 49 967u. The original ligand, IX1 (Figure 2) is observed in the complex with PTP1B[20].

**Fig. 1 Three dimensional structure of PTP1B**

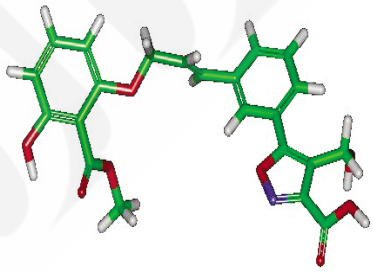

**Fig. 2 The Structure of IX1**

Active center and the residues of active area were defined according to the position of original ligand. 7 residues selected are shown in Figure 3, which are Arg254, Gln262, Tyr46, Asp181, Ser216, Phe182, and Arg221.

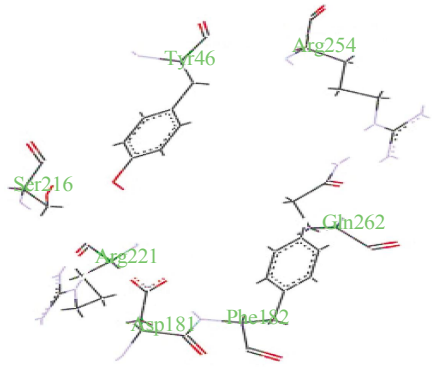


**Fig. 3 Defined binding pocket**

### 1.2 The preparation of ligands

A library of natural products containing 42 296 molecules was constructed based on two databases. Firstly, the National Compound Resource Center(http://www.chemicallibrary.org.cn/) provided a total of 6988 small molecules, including 4 406 unknown active natural products obtained from plants and microorganisms, 2 080 various structural types of natural products offered by BioBioPha company and 502 monomeric compounds isolated from natural plants. Besides, Baihan Biological Technology Co. Ltd. (http://www.baihansw.com/) constructed a library containing 35 308 compounds coming from traditional Chinese Medicine Database(TCM Database@Taiwan)[21], which contains approximately 30 000 compounds coming from 443 kinds of Chinese herbs, and is currently the largest non-commercial TCM database.

All of the small molecules included in the docking library were subjected to the calculation of characteristic value, energy optimization, generating three-dimensional coordinates, assignment of hydrogen and Gasteiger-Marsilli charges, filtering according to the Lipinski's Rule of Five[22]. Saving the docking library preliminary screened with a total of 14 837 molecules for subsequent screening.

### 1.3 Determination of docking parameters

The original ligand was extracted from 1XBO, followed by energy optimization. Then, the ligand was reconnected back to the active center of the receptor (*i.e.*, the cavity in which it is located) within the LibDock module. Central coordinates and the radius of active sphere were set at the same time. Next, the Root Mean Square Deviation (RMSD) between the molecular conformations after docking and the conformation of original ligand was calculated. The docking parameter is considered reasonable if RMSD ≤2Å. After constantly adjusting the position and size of the active sphere and molecular docking calculations, the center coordinates (32.2, 28.32, 22.47) and radius (11.9Å) were adjusted, with RMSD value of 1.3086Å. The LibDock scoring and the -CDOCKER Interaction Energy between original ligand and PTP1B are 147.320 and 59.293 kJ·mol$^{-1}$, respectively, which could be used as controls for binding affinities level of potential PTP1B inhibitors.

### 1.4 Investigation of docking algorithm and scoring functions

57 PTP1B inhibitors with diversity and obvious gradient activity($IC_{50}$ value of 1.7 nmol/L～271.2 μmol/L) were selected from Binding Database (http://www.bindingdb.org/) to investigate the feasibility of docking method and scoring functions. Docking simulations of these 57 molecules within Libdock were carried out. The scorings were calculated by 8 kinds of scoring functions, LibDockScores, LigScore1, LigScore2, PLP1, PLP2, Jain, PMF, and PMF04. The scatter plots of 8 scoring functions and p$IC_{50}$ were obtained and the linear regression coefficients were calculated.

### 1.5 Virtual screening based on molecular docking

Semi flexible molecular docking was performed in the LibDock module. The first screened molecules in the docking library were docked to PTP1B in turn. Using scoring of the original ligand as a threshold, 1 678 molecules with LibDockScore above 140 were selected.

Then CDOCKER module based on CHARMm semi flexible docking program was employed. High temperature kinetic was used to generate small molecules conformation set. CHARMm forcefield was added and Momany-Rone charges were assigned to all ligands. Electrostatic interactions were taken into consideration. The search steps were adopted 1 000 with search dynamic target temperature of 1 000℃. Conformations were optimized by the method of simulated annealing[23] from 2 000 steps to 5 000 steps, and temperature was cooling to 300℃ from 700℃. Each molecule had 10 conformations finally, but only one with the lowest energy was selected. Of which 11 molecules with -CDOCKER Interaction Energy above 59 kJ·mol$^{-1}$ were selected for further researches.

### 1.6 Predictions of pharmacokinetic characteristics and toxicological properties

ADMET refers to *in vivo* absorption, distribution, metabolism, excretion and toxicity properties of molecules. ADMET properties predictions could not only help to screen compounds, but also evaluate the effect of structure optimization.

Pharmacokinetic characteristics of compounds were chosen in this study, including Human Intestinal Absorption (HIA), Solubility, Blood Brain Barrier permeability (BBB), Cytochrome P450 2D6 inhibitory activity (CYP2D6), Plasma Protein Binding rate (PPB), and Hepatotoxicity. Each feature is predicted by corresponding model. The HIA model validated by external data was used to predict intestinal absorption after oral administration. The water solubility model used linear regression to predict the water soluble

properties of compounds at 25℃. The BBB model contains a quantitative regression model for the prediction of blood-brain barrier permeability and 95% or 99% confidence intervals, which was verified by 881 central nervous system compounds in CMC database [24]. The CYP2D6 model was used to predict enzyme inhibitory activity of the compounds according to modified Bayesian fitting method and one by one cross validation method. The construction method of PPB and hepatotoxicity model model are similar to that of the CYP2D6 inhibitory model. The screening criteria for the above pharmacokinetic parameters are shown in Table 1.

The selected models of toxicological properties prediction included Ames Mutagenicity, Rat Oral $LD_{50}$, Aerobic biodegradability, and Rodent Carcinogenicity. Cross validated quantitative structure toxicity relationships (QSTR) models[25] based on the molecular 2D structures was used to predict these properties and evaluate various toxicity predictions. Computed probability values of 0.00–0.30, 0.30–0.70, 0.70–1.00 were regarded as non-toxic, indeterminate and toxic, respectively.

**Table 1 Pharmacokinetic parameters screening criteria**

| Models | Level | | | | | |
|---|---|---|---|---|---|---|
| | *0* | *1* | *2* | *3* | *4* | *5* |
| HIA | Good | Moderate | Low | Very low | – | – |
| Solubility | Extremely low | No, very low, but possible | Yes, low | Yes, good | Yes, optimal | No, too soluble |
| BBB | Very high | High | Medium | Low | – | – |
| CYP2D6 | Non-inhibitor | Inhibitor | – | – | – | – |
| PPB | Binding < 90% | Binding > 90% | Binding > 95% | – | – | – |
| Hepatotoxicity | Nontoxic | Toxic | – | – | – | – |

### 1.7 Assay for PTP1B inhibition

The *in vitro* inhibition ability of compound *10* to PTP1B with the *p*NPP as substrate was tested. PTP1B, purchased from Sino Biological Inc. (95% purity), was diluted to an optimal concentration 0.25 g/L with enzyme dilution buffer(25 mmol/L HEPES, 50 mmol/L NaCl, 5 mmol/L dithiothreitol and 2.5 mmol/L EDTA, pH 7.2). A typical 188 μl reaction system contained 5 μl BSA (5 g/L), 51 μl $H_2O$, 4 μl PTP1B, 108 μl buffer, and 20 μl series of gradient concentrations (between 1 μmol/L and 10 000 μmol/L) of compound *10* (purchased from TopScience Corporation, 90% purity) dissolved in DMSO. Subsequently, the mixture had been incubated at 37℃ for 15 min. The enzyme reaction was initiated by the addition of 12 μl *p*NPP (1.5 g/L). After 30 min at 37℃, the reaction was terminated by 40 μl $Na_2CO_3$ (2 mol/L). 50 μl each of blank was transferred into quadruplicate wells. $Na_3VO_4$ was used as a positive control. The absorbance at 405 nm was measured by Thermo Multiskan Ascent Microplate assay to quantify the *p*-nitrophenyl produced. The nonenzymatic hydrolysis of 12 μl *p*NPP was corrected for the error in absorbance at 405 nm obtained in the existence of PTP1B enzyme. The inhibition percentage was calculated based on the following equation:

$$i=(1-[(OD-OD_0)/(OD_t-OD_0)])\times 100\%$$

where $OD$ is the absorbance of tested compound, $OD_t$ is the absorbance of negative control and $OD_0$ is the absorbance of blank group.

## 2 Results and discussion

### 2.1 Investigation of docking algorithm and scoring functions

In order to verify the feasibility of scoring algorithm and scoring functions, the linear regression coefficients of 8 models were calculated. As a result, a good linear correlation ($R^2$ is 0.81914 or 0.81661) between the experimental value p$IC_{50}$ and LibDockScore or PLP2 is observed, higher than those of the other 6 models. Figure 4 shows the scatter diagrams between p$IC_{50}$ and LibDockScore or PLP2.

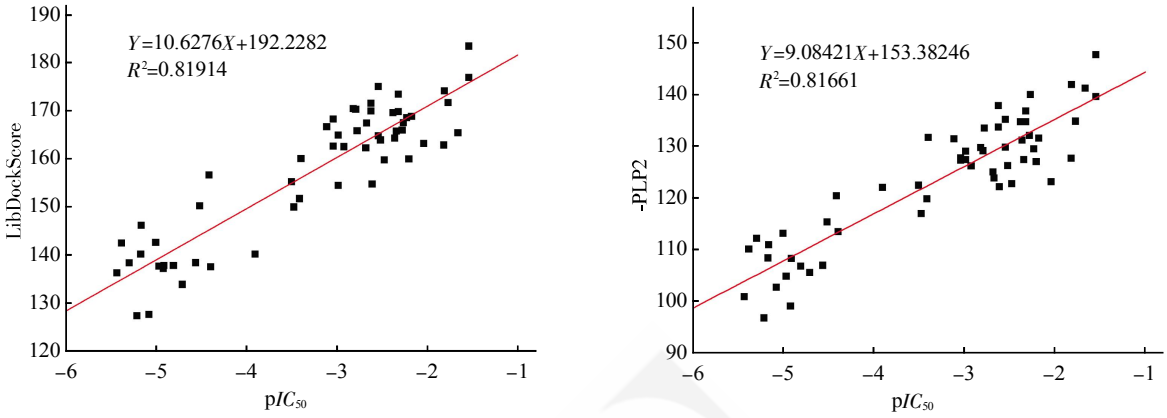


**Fig. 4 The scatter diagrams between $pIC_{50}$ and LibDockScore or PLP2**

## 2.2 Result of virtual screening

11 molecules with high scorings obtained after 3 rounds of screening were shown in Table 2. Their structural formulas were attached to Figure S1.

According to Table 2, there is not much difference in scorings among these compounds, and -CDOCKER Interaction Energy of all candidate inhibitors are higher than that of IX1. What's more, it can be concluded that all the molecules have benzene ring or hexatomic ring and at least two hydroxyls. The middle part or the side chain of those 11 molecules are approximately structurally similar, and could be considered as nearly as linear structure.

**Table 2 Docking function scorings of original ligand and 11 molecules**

| Compounds | Molecular Formula | LibDockScore | -PLP2 score | -CDOCKER interaction energy/(kJ•mol$^{-1}$) |
|---|---|---|---|---|
| IX1 | $C_{22}H_{19}NO_8$ | 147.320 | 115.76 | 59.293 |
| *1* | $C_{29}H_{40}O_6$ | 157.609 | 115.28 | 70.313 |
| *2* | $C_{29}H_{39}O_5$ | 145.613 | 104.69 | 66.466 |
| *3* | $C_{23}H_{28}O_6$ | 147.831 | 113.24 | 62.409 |
| *4* | $C_{24}H_{29}O_5$ | 145.505 | 121.70 | 61.466 |
| *5* | $C_{29}H_{40}O_6$ | 142.089 | 100.82 | 67.116 |
| *6* | $C_{22}H_{26}O_6$ | 145.043 | 115.41 | 60.429 |
| *7* | $C_{21}H_{27}O_4^-$ | 143.840 | 87.820 | 66.818 |
| *8* | $C_{21}H_{24}O_6$ | 141.363 | 111.81 | 60.918 |
| *9* | $C_{21}H_{22}O_6$ | 140.050 | 118.37 | 60.659 |
| *10* | $C_{20}H_{30}O_5$ | 141.021 | 97.970 | 62.268 |
| *11* | $C_{20}H_{37}NO_4$ | 141.142 | 86.180 | 65.751 |

## 2.3 Predictions of pharmacokinetic characteristics and toxicological properties

The pharmacokinetic parameters and toxicity parameters of these 11 molecules were predicted. Pharmacokinetic scorings and optimal prediction space (OPS) results are listed in Table 3 and Table 4. As shown in Table 3, the levels of hepatotoxicity predictions of compounds *3*, *4*, *6*, *8*, and *9* are 1, indicating these compounds have obvious hepatotoxicity. Compounds *1*, *2*, *5* are also eliminated due to reliable high carcinogenic possibility according to Table 4. Of these molecules, 3 candidate inhibitors

*7*, *10* and *11* with high scorings and good properties were screened out, and their structural formulas are shown in Figure 5.

Para-benzoquinone compound *7* was extracted and isolated for the first time from *Hypericum erectum* by An *et al.*[26] in 2002. In 2003, Hu *et al.*[27] firstly demonstrated that compound *7* has significant PTP1B inhibitory activity through enzymatic assay in accordance with our screening results, which also indicated that our screening method is highly accurate. Isocoumarins derivatives *10* was firstly extracted from *Ononis pubescens* by Barrero *et al.*[28] in 1994. PTP1B inhibitory activity of it's structurally similar coumarin fluorescent molecules was reported[29], so that of 10 could be speculated. Clavepictine analogue *11* has not been reported before.

**Table 3 Pharmacokinetic parameters of original ligand and 11 molecules**

| Compounds | BBB | HIA | Solubility | Hepatotoxicity | CYP2D6 | PPB |
|---|---|---|---|---|---|---|
| IX1 | 4 | 2 | 3 | 1 | 0 | 0 |
| *1* | 4 | 1 | 2 | 0 | 0 | 2 |
| *2* | 4 | 1 | 2 | 0 | 0 | 2 |
| *3* | 4 | 0 | 3 | 1 | 1 | 1 |
| *4* | 4 | 1 | 2 | 1 | 0 | 2 |
| *5* | 4 | 2 | 2 | 0 | 0 | 2 |
| *6* | 4 | 0 | 2 | 1 | 1 | 1 |
| *7* | 2 | 0 | 2 | 0 | 0 | 0 |
| *8* | 3 | 0 | 3 | 1 | 0 | 0 |
| *9* | 3 | 0 | 3 | 1 | 0 | 0 |
| *10* | 3 | 0 | 4 | 0 | 0 | 0 |
| *11* | 4 | 1 | 2 | 0 | 1 | 1 |

**Table 4 Toxicity predictions of original ligand and 11 molecules**

| Compounds | Ames mutagenicity | | Rat Oral $LD_{50}$ Log(1/Moles) | | Aerobic biodegradability | | Rodent carcinogenicity | |
|---|---|---|---|---|---|---|---|---|
| | Prediction | OPS | Prediction | OPS | Prediction | OPS | Prediction | OPS |
| IX1 | 0.000 | T&T[1)] | 0.777 | T&T | 0.000 | F&F[2)] | 0.350 | T&T |
| *1* | 0.000 | T&T | 3.419 | F&F | 0.000 | F&F | 1.000 | T&T |
| *2* | 0.000 | T&T | 1.129 | F&F | 0.000 | F&F | 1.000 | T&T |
| *3* | 0.000 | F&F | 1.118 | F&T[3)] | 1.000 | F&F | 1.000 | T&T |
| *4* | 0.016 | T&T | 1.077 | T&T | 0.000 | F&F | 0.998 | T&T |
| *5* | 0.000 | T&T | 3.310 | F&F | 0.005 | F&F | 1.000 | T&T |
| *6* | 0.002 | T&T | 1.539 | T&T | 0.953 | F&F | 0.115 | T&T |
| *7* | 0.000 | F&F | 0.957 | F&F | 0.000 | F&F | 0.000 | F&F |
| *8* | 0.002 | T&T | 1.431 | T&T | 1.000 | F&F | 0.375 | T&T |
| *9* | 0.011 | T&T | 1.443 | T&T | 0.000 | F&F | 0.508 | T&T |
| *10* | 0.000 | T&T | 2.527 | F&F | 0.000 | F&F | 0.000 | F&F |
| *11* | 0.000 | T&T | 2.129 | T&T | 1.000 | F&F | 1.000 | F&F |

[1)] T&T indicates the compounds are located in the optimal prediction space of the models, and the prediction results are credible; [2)] F&F indicates the models don't apply to the compounds, and predictions are not credible; [3)] F&T indicates compounds are located within the limits of optimal prediction space of the models, and the prediction results are credible.

## 2.4 Analysis of the binding mode of candidate inhibitors in the active site of PTP1B

Binding model research was operated to gain structural insight into the inhibitory mechanisms for the identified PTP1B inhibitors. Binding orientations of all the inhibitors were observed.

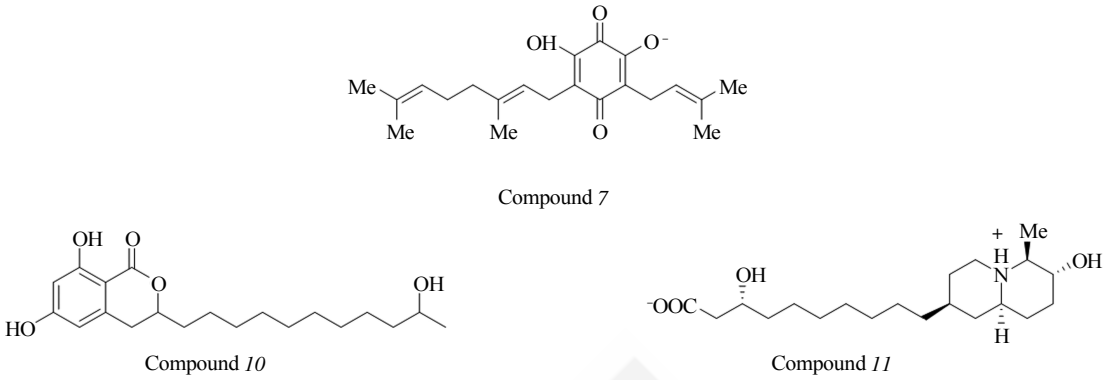


**Fig. 5　Chemical structures of candidate inhibitors**

The catalytic active sites of the PTP1B involving dephosphorylation reaction include: (1) the first active site, which consists of amino acid residues from 214 to 221, namely His214- Cys215- Ser216- Ala217- Gly218- Ile219- Gly220- Arg221, of which Cys215 and Arg221 play key roles in the process of catalysis[30]. (2) The second active site, secondary aryl phosphate binding site[31], which includes Tyr20, Arg24, Ala27, Phe52, Arg254, Met258 and Gly259. That have extremely weak interactions, and no catalytic activity. (3) WPD loop, including residues from 179–187, of which Phe182 acts as a switch. $\pi$-$\pi$ conjugate is formed between benzene ring of Phe182 and that of Tyr to fix the substrate[32]. (4) YRD loop, composed of Tyr46-Arg47-Asp48[33]. (5) The linker, where located residues such as Gln262, normally forms hydrogen bonds by amidic nitrogen with certain groups of inhibitors[34].

Docking drawings of IX1, candidate inhibitors *7*, *10* and *11* with PTP1B are shown in Figure 6. It's seen that the 3 small molecules are all docked into the cavity, in which the original ligand is located. Figure 7 shows the two-dimensional representation of IX1 and candidate inhibitors in the active sites of PTP1B.

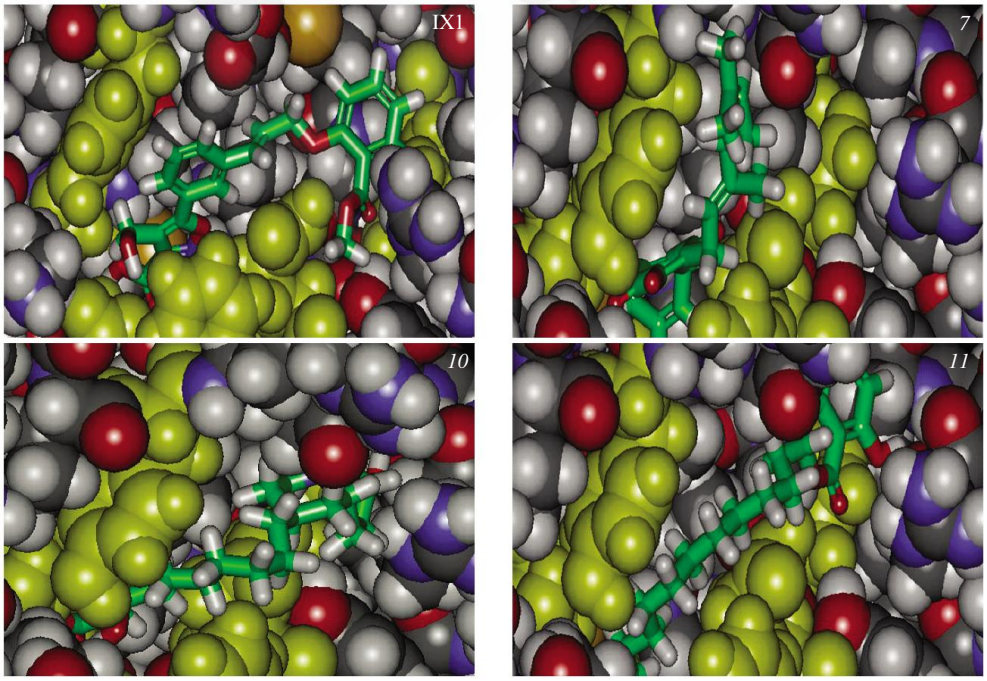


**Fig. 6　Figure of IX1 and 3 candidate inhibitors (7, 10, 11) in the active site of PTP1B**

Yellow: Defined binding pocket. Green stick: Inhibitors. The others: Other parts of PTP1B.

As shown in Figure 7a, carboxyl group at the one end of IX1 forms hydrogen bonding interactions with Arg221, Ser216 and Gly220, mainly occupying the first site. Hydroxyl oxygen on the terminal phenyl ring forms hydrogen bonding with Arg24 and Arg254, which are parts of the second site and help in exhibiting selectivity and specificity of binding. Besides, the phenyl ring of IX1 makes a good $\pi$-$\pi$ stacking interaction with that of Arg24 residue. As is expected, IX1 binds both site 1 and site 2 of PTP1B. Other residues around the ligand such as Phe182, involved in the WPD loop closure, is stabilized by van der Waals contacts, and Tyr46 of YRD loop are mainly involved in electrostatic or polar interactions.

Figure 7b indicated that the benzene ring of compound *7* is embedded into the first site and YRD loop. Hydroxyl and carbonyl groups form the hydrogen bond interactions with the key residues of above two sites, such as Arg221, Tyr46 and so on. 12 amino acid residues, Gln262, Phe182, Gly220, Gln266, Ile219, Ser222, Gly218, Cys215, Arg47, Asp48, Ser216, and Asp181, from different active sites connected with *7* primarily by van der Waals interactions, electrostatic or polar interaction.

Figure 7c revealed the binding mode of compound *10* with PTP1B. Arg221 and Ser216 are located at the first site of PTP1B, in which the catalytic pocket is relatively narrow. Because of the long carbon chain, compound *10* can extend easily deep into the catalytic pocket, forming hydrogen bond and electrostatic or polar interactions with key residues of this site. On the other hand, Arg221 plays a vital role in the process of catalyzing substrate dephosphorylation. The formation of hydrogen bond with acceptor strengthens the combination of enzyme and inhibitors. Arg24 and Arg254 belonging to the second site have a weak binding effect and no catalytic activity. One hydrogen bond is established between the lactone structure of compound *10* and Arg24. Arg254 also receives one hydrogen bond from the hydroxyl group on the benzene ring. There also existed $\pi$-$\sigma$ bond between benzene and Arg24, that is, $\pi$-$\pi$ interactions. Gln262 is situated at the junction between the first site and the second site. Moreover, Gln262 is related to the hydrolysis of the intermediates. As exhibited in Figure 7c, the amide bonds of Gln262 connected with the lactone structure of compound *10* by one hydrogen bond. Furthermore, presence of

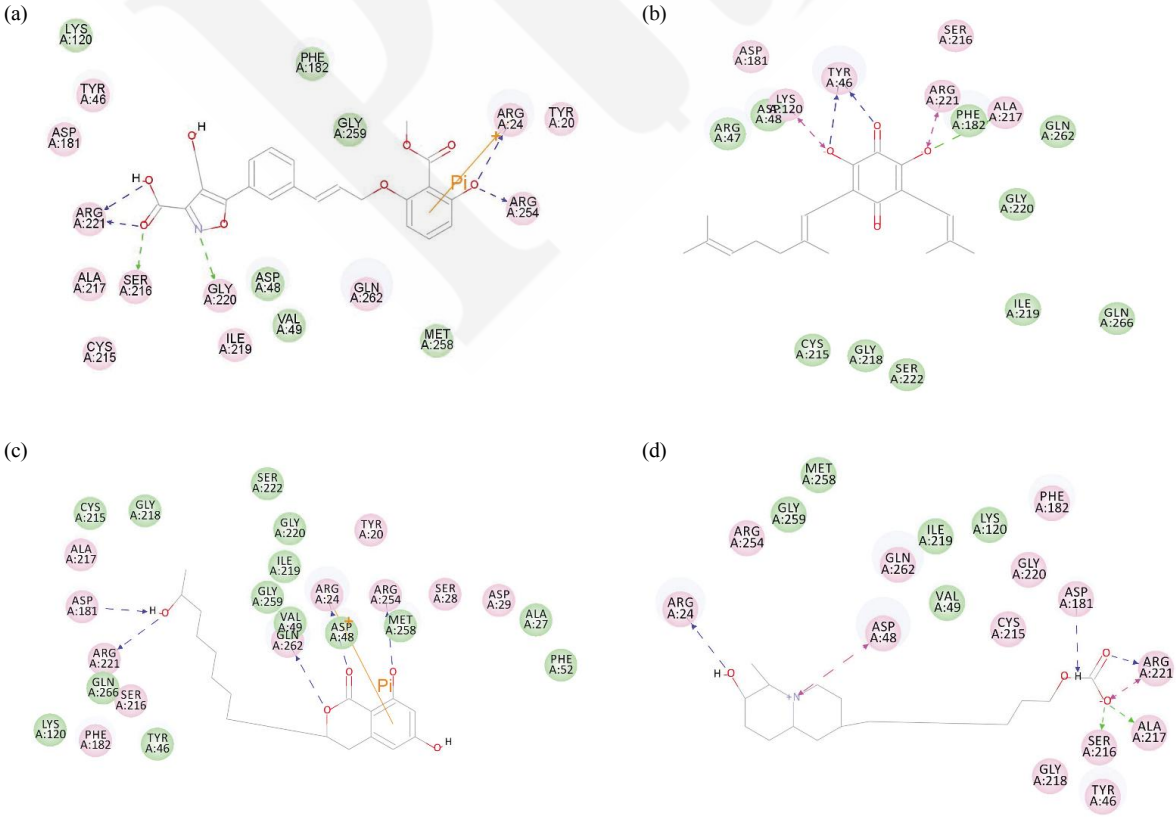


**Fig. 7 Two dimensional representation of interactions between inhibitors and PTP1B**

(a) IX1. (b) Compound *7*. (c) Compound *10*. (d) Compound *11*.

Tyr46 and Phe182 in YRD loop and WPD loop respectively, coplanar with the phenyl ring suggested the possible hydrophobic interactions between compound *10* and PTP1B. On the basis of the above analysis, it can be speculated that compound *10*, fitting the specific second active site very well besides the first active site, has a strong and selective activity. Besides, terminal benzene of compound *10* provides two hydroxyl groups, which is similar to that of the original ligand. Quite coincidentally, it is exactly the same binding mode that there is one hydrogen bond received by Arg254, and one $\pi$-$\sigma$ bond leading to $\pi$-$\pi$ interactions between benzene and Arg24 compared with IX1.

Figure 7d shows that compound *11* are conjugated with PTP1B mainly by hydrogen bonds. Terminal carboxyl of long carbon chain of compound *11* is located within the first active site of PTP1B, where Arg221, Ser216 and Ala217 residues are found to obtain 4 H-Bonds from carboxyl oxygen. There exists only one residue from the second site, Arg24, having the hydrogen bonding with the hydroxyl group extending out from the hexatomic ring. At the same time, nitrogen on the hexatomic ring and hydroxyl near to carboxyl were also observed to form one hydrogen bond with Arg48 of YRD loop and Asp181 of WPD loop, respectively. In addition, the compound *11* is linked with 12 bonding sites by electrostatic or polar interactions, which are Arg254, Gln262, Phe182, Tyr46, Gly259, Met258, Ile219, Lys120, Val49, Cys215, Gly220, and Gly218, from diverse binding sites. IX1 and compound *10* can simultaneously occupy two sites while *11* mainly occupy the first site, weakly combing with the second site. Compared with IX1 and *10*, *11* has a carboxyl group at the end, lack of benzene ring structure. So compound *11* is speculated to have relatively weak selectivity towards PTP1B.

IX1 was firstly designed and synthesized by Zhao *et al*.[20] in 2004. In this paper, the molecular docking, ADMET, and binding mode were introduced to find new inhibitors. Compounds *7*, *10* and *11* are identified by applying a computer aided drug design protocol, involving the structure-based virtual screening with molecular docking from constructed natural product library. Of which, the PTP1B inhibitory activity of compound *7* has been experimentally confirmed in the previous study[27], while that of compounds *10* and *11* have not been reported. In 2013, Sun [35] reported PTP1B inhibitory activity of coumarin derivatives *12* (Figure 8) with $IC_{50}$ values of 49.17 μmol/L, structure of which is too large to enter the first site of PTP1B, but can form hydrogen bonds and $\pi$-$\sigma$ bond with the second active site. Compared with compound *12*, compound *10* possesses similar coumarin ring, but it can bind with the first site and the second site at the same time. These results support the hypothesis that *10* would have higher affinity on the active site of PTP1B. Deep researches will be carried out in further works.

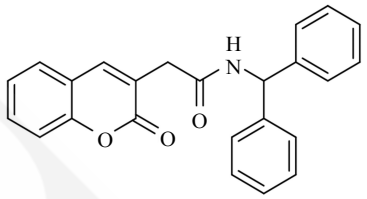


Compound *12*

**Fig. 8 Chemical structure of compound 12 [35]**

## 2.5 Enzymatic assay and $IC_{50}$ determination

The inhibitory activity of compound *10* on PTP1B enzyme was operated. Inhibition rate and $IC_{50}$ were shown in Table 5. As seen from table 5, compound *10* is the newly identified PTP1B inhibitor with $IC_{50}$ values of (74.58 ±1.235) μmol/L though lower than that of $Na_3VO_4$ and in the same order of magnitude compared that of *12*. However, compound *10* would have good biocompatibility and low toxic side effects, so that can be considered as a new inhibitor scaffold for further optimization.

**Table 5 PTP1B inhibitory activity of compound 10 (n=4)**

| $c_{compound10}$/(μmol•L$^{-1}$) | $i$/% | $IC_{50}$/(μmol•L$^{-1}$) |
|---|---|---|
| 10 000 | 93.64±1.927 | |
| 5 000 | 95.63±10.593 | |
| 2 500 | 91.32±1.731 | |
| 1 000 | 80.30±5.812 | |
| 500 | 81.19±2.004 | |
| 250 | 50.87±5.928 | |
| 100 | 49.02±3.505 | 74.58±1.235 |
| 50 | 39.53±3.575 | |
| 25 | 37.93±2.768 | |
| 10 | 36.34±4.850 | |
| 5 | 17.18±5.546 | |
| 2.5 | 17.20±6.316 | |
| 1 | 13.76±5.938 | |
| $Na_3VO_4$ [1)] | – | 9.495±1.163 |

[1)] Used as positive controls.

## 3 Conclusion

11 highly scored molecules have been screened from constructed natural product library containing 42 296 molecules by molecular docking. Afterwards 3 potential inhibitors are identified combined with simulation of pharmacokinetic and toxicological properties, namely, parabenzoquinone compound *7*, isocoumarins derivative 10 and Clavepictine analogue *11*, of which *10* and *11* are structurally diverse and their inhibitory activities of PTP1B have not been reported before. The binding mode analysis with molecular docking simulation shows *10* and *11* can be stabilized by multiple hydrogen bonds, van der Waals contacts, electrostatic or polar interaction, indicating both of them possess great PTP1B inhibitory activity. Enzymatic assay showed that the $IC_{50}$ of *10* against PTP1B is (74.58 ±1.235) μmol/L, so it could be potential diabetes drug.

**Acknowledegments** We are grateful to Prof. DAI Rongji of Beijing Institute of Technology for providing help and access to computer software such as Discovery Studio3.1 during the process of study.

**Supplementary material** Figure S1 is available at paper online(http://www.pibb.ac.cn).

### References

[1] Cicirelli M F, Tonks N K, Diltz C D, *et al*. Microinjection of a protein-tyrosine-phosphatase inhibits insulin action in *Xenopus oocytes*. Proc Natl Acad Sci USA, 1990, **87**(14): 5514−5517

[2] Elchebly M, Payette P, Michaliszyn E, *et al*. Increased insulin sensitivity and obesity resistance in mice lacking the protein tyrosine phosphatase-1B gene. Science, 1999, **283**(5407): 1544−1548

[3] Zhou M, Zhang W, Cheng Y H, *et al*. Molecular docking and 3D-QSAR studies on protein tyrosine phosphatase 1B inhibitors. Acta Chim Sinica, 2005, **63**(23): 2131−2136

[4] Wiesmann C, Barr K J, Kung J, *et al*. Allosteric inhibition of protein tyrosine phosphatase 1B. Nat Struct Mol Biol, 2004, **11**(8): 730−737

[5] 刘 霞, 冯长根. 蛋白酪氨酸磷酸酶 -1B 抑制剂研究进展. 科技导报, 2012, **30**(10): 72−79
Liu X, Feng C G. Sci Technol Rev, 2012, **30**(10): 72−79

[6] Zhao X, Wang S, Xu X H, *et al*. Molecular simulation study on the enediyne ring chromophore releasing mechanism from the Holo-NCS protein. Acta Chim Sinica, 2009, **67**(16): 1835−1838

[7] Oh W K, Lee C H, Lee M S, *et al*. Antidiabetic effects of extracts from Psidium guajava. J Ethnopharmacol, 2005, **96**(3): 411−415

[8] 刘美凤, 蒋利荣, 刘华鼐,等. 番石榴叶抗Ⅱ型糖尿病活性成分的虚拟筛选. 华南理工大学学报(自然科学版), 2011, **39**(3): 28−31
Liu M F, Jiang L R, Liu H N, *et al*. Journal of South China University of Technology (Social Science Edition), 2011, **39**(3): 28−31

[9] Park H, Bhattarai B R, Ham S W, *et al*. Structure-based virtual screening approach to identify novel classes of PTP1B inhibitors. Eur J Med Chem, 2009, **44**(8): 3280−3284

[10] Joshi P, Deora G S, Rathore V, *et al*. Identification of ZINC02765569: a potent inhibitor of PTP1B by vHTS. Med Chem Res, 2013, **22**(1): 28−34

[11] Vyas B, Silakari O, Kaur M, *et al*. Integrated pharmacophore and docking-based designing of dual inhibitors of aldose reductase (ALR2) and protein tyrosine phosphatase 1B (PTP1B) as novel therapeutics for insulin-resistant diabetes and its complications. J Chemom., 2015, **29**(2):109−125

[12] Wang M, Li X, Dong L, *et al*. Virtual screening, optimization, and identification of a novel specific PTP-MEG2 Inhibitor with potential therapy for T2DM. Oncotarget, 2016, **7**(32):50828−50834

[13] Chandra S, Pandey J, Tamrakar A K, *et al*. Multiple machine learning based descriptive and predictive workflow for the identification of potential PTP1B inhibitors. Journal of Molecular Graphics & Modelling, 2016, **71**: 242−256

[14] Lantz K A, Hart S G E, Planey S L, *et al*. Inhibition of PTP1B by trodusquemine (MSI-1436) causes fat-specific weight loss in diet-induced obese mice. Obesity, 2010, **18**(8): 1516−1523

[15] Swarbrick M M, Havel P J, Levin A A, *et al*. Inhibition of protein tyrosine phosphatase-1B with antisense oligonucleotides improves insulin sensitivity and increases adiponectin concentrations in monkeys. Endocrinology, 2009, **150**(4): 1670−1679

[16] Huyer G, Liu S, Kelly J, *et al*. Mechanism of inhibition of protein-tyrosine phosphatases by vanadate and pervanadate. J Biol Chem, 1997, **272**(2): 843−851

[17] Shen K, Keng Y, Wu L, *et al*. Acquisition of a specific and potent PTPIB inhibitor from a novel combinatorial library and screening procedure. J Biol Chem, 2001, **276**(50): 47311−47319

[18] Inc. A S. Discovery studio modeling environment, Release 2.5.5 [CP/OL]. San Diego: Accelrys Software Inc, 2010 [2017-3-12]. http://accelrys.com/

[19] Berman H M, Westbrook J, Feng Z, *et al*. The protein data bank. Nucleic Acids Res, 2000, **28**(1): 235−242

[20] Zhao H Y, Liu G, Xin Z L, *et al*. Isoxazole carboxylic acids as protein tyrosine phosphatase 1B (PTP1B) inhibitors. Bioorg Med Chem Lett, **14**(22):5543−5546

[21] Chen C Y. TCM Database@Taiwan: the world's largest traditional chinese medicine database for drug screening in silico. Plos One, 2011, **6**(1): e15939

[22] 田 盛. 基于中药资源的计算机辅助药物分子设计[D]. 江苏: 江苏大学, 2014
Tian S. Computer-aided Drug Design Based on Traditional Chinese Medicines[D]. JiangSu: Soochow University, 2014

[23] Goodsell D S, Olson A J. Automated docking of substrates to

proteins by simulated annealing. Prot Struct Funct Genet, 1990, **8**(3): 195-202

[24] Egan W J, Lauri G. Prediction of intestinal permeability. Adv Drug Delivery Rev, 2002, **54**(3): 273-289

[25] Gombar V K, Enslein K, Blake B W. Assessment of developmental toxicity potential of chemicals by quantitative structure-toxicity relationship models. Chemosphere, 1995, **31**(1):2499-2510

[26] An T Y, Shan M D, Hu L H, *et al*. Polyprenylated phloroglucinol derivatives from *Hypericum erectum*. Phytochemistry, 2002, **59**(4): 395-398

[27] Hu L, Li J, Ye Q, *et al*. Para-benzoquinone compounds isolated from *Ardisia* and *Forsythia* as protein tyrosine phosphatase 1B inhibitors: CN, 1521157. 2004-08-18

[28] Barrero A F, Rodrí guez E C I, Planelles F. Alkylresorcinols and isocoumarins from *Ononis pubescens*. Phytochemistry, 1994, **35**(2): 493-498

[29] Holmes C P, Macher N, Grove J R, *et al*. Designing better coumarin-based fluorogenic substrates for PTP1B. Bioorg Med Chem Lett, 2008, **18**(11): 3382-3385

[30] Rondinone C M, Trevillyan J M, Clampit J, *et al*. Protein tyrosine phosphatase 1B reduction regulates adiposity and expression of genes involved in lipogenesis. Diabetes, 2002, **51**(8): 2405-2411

[31] Hsu M, Meng T. Enhancement of insulin responsiveness by nitric oxidemediated inactivation of protein-tyrosine phosphatases. J Biol Chem, 2010, **285**(11): 7919-7928

[32] Shinde R N, Sobhia M E. Geometrical criteria for characterizing open and closed states of WPD-loop in PTP1B. J Mol Struct, 2012, **1017**(23): 79-83

[33] Johnson T O, Ermolieff J, Jirousek M R. Protein tyrosine phosphatase 1B inhibitors for diabetes. Nat Rev Drug Discovery, 2002, **1**(9): 696-709

[34] 赵丹. PTPlB 抑制剂结合过程及筛选方案的研究[D]. 大连: 大连理工大学, 2015
Zhao D. Studies of the Inhibitor Binding Process on PTP1B and the Screening Approach[D]. Dalian: Dalian University of Technology, 2015

[35] 孙程. PTP1B 潜在抑制剂 - 香豆素衍生物的合成及体外活性检测[D]. 天津: 南开大学, 2013
Sun C. Synthesis of Coumarin Derivatives and Biological Evaluation as Potential PTP1B Inhibitors in Vitro [D]. Tianjin: Nankai University, 2013

# 基于天然产物的蛋白酪氨酸磷酸酶 1B 抑制剂的虚拟筛选

张 倩[1] 甘 强[1]* 刘 霞[2] 陈 曦[1] 冯长根[1]*

([1] 北京理工大学爆炸科学与技术国家重点实验室，北京 100081；[2] 中国农业大学理学院，北京 100193)

**摘要** 蛋白酪氨酸磷酸酶 1B (protein tyrosine phosphatase 1B，PTP1B) 是治疗Ⅱ型糖尿病的靶点之一，筛选 PTP1B 抑制剂具有十分重要的意义．本文采用分子对接虚拟筛选方法，构建共含有 42 296 个小分子的天然产物库，分别与 PTP1B 靶点蛋白进行分子对接，以原配体的结合能量为阈值，经过三轮筛选选取打分值高于阈值的小分子进行药代动力学参数和毒性参数预测，最终筛选出 3 个 PTP1B 抑制剂，对苯醌类化合物 *7*、异香豆素类衍生物 *10* 和 Clavepictine 类似物 *11*．结合方式研究表明，3 个候选抑制剂类药性良好，均具有较好的 PTP1B 抑制活性，其中化合物 *10* 和 *11* 的 PTP1B 抑制活性未见报道．对化合物 *10* 进行体外抑制活性检测，其 $IC_{50}$ 为(74.58±1.23) μmol/L，可作为潜在Ⅱ型糖尿病治疗药物．

**关键词** 蛋白酪氨酸磷酸酶 1B 抑制剂，虚拟筛选，天然产物，药代动力学特性，毒理性质，氢键，抑制活性

**学科分类号** Q5，Q81，O69 **DOI**: 10.16476/j.pibb.2018.0020

* 通讯联系人.

甘 强. Tel: 010-68913770, E-mail: ganqiang@bit.edu.cn

冯长根. Tel: 010-68912941, E-mail: cgfeng@cast.org.cn

收稿日期：2018-01-15，接受日期：2018-03-09

# Supplements

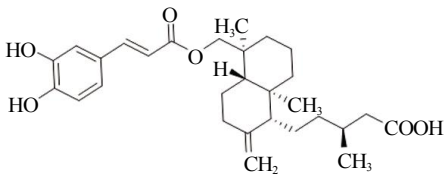

Compound *1*

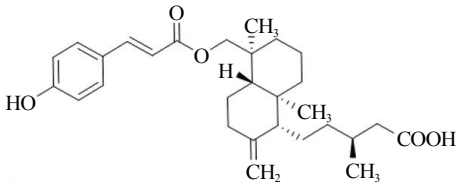

Compound *2*

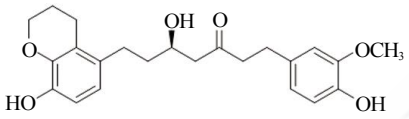

Compound *3*

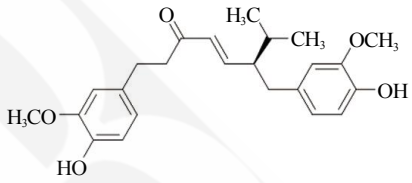

Compound *4*

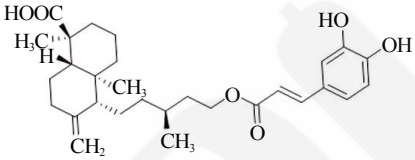

Compound *5*

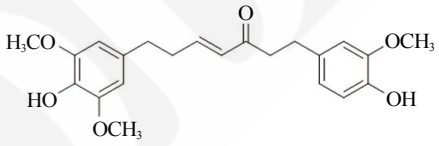

Compound *6*

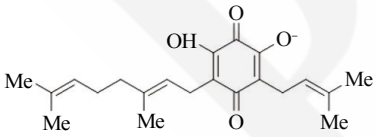

Compound *7*

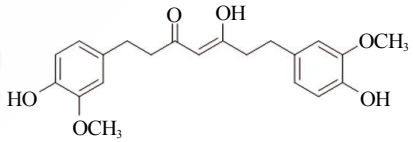

Compound *8*

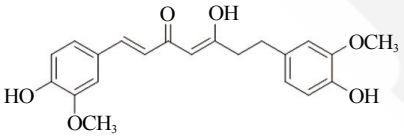

Compound *9*

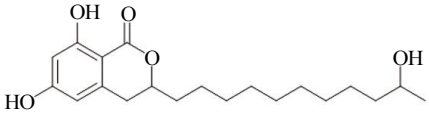

Compound *10*

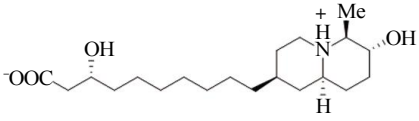

Compound *11*

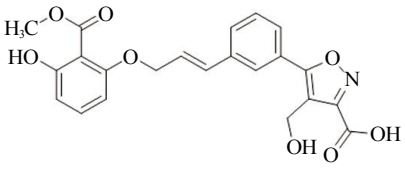

IX1

**Fig. S1 The structures of 11 molecules**